Chem Rev Lett 8 (2025) 441-447

Research Article

Chemical Review and Letters
journal homepage: www.chemrevlett.com
ISSN (online): 2645-4947 (print) 2676-7279

Preparation and characterization of a new nanomachine as interlocked molecule

Abdullah Najdhashemi[1], Samad Bavili Tabrizi[1]*, Mirzaagha Babazadeh[1]

[1]*Department of Chemistry, Faculty of Science, Tabriz Branch, Islamic Azad University, Tabriz, I.R. IRAN*

ARTICLE INFO

Article history:
Received 29 December 2024
Received in revised form 11 March 2025
Accepted 21 March 2025
Available online 23 May 2025

Keywords:
Nanomachine
Macrocycles
Crown ethers
Rotaxane
Mechanically interlocked molecules.

ABSTRACT

The rotaxane configuration, among the various interlocked molecular structures, is recognized as a flexible foundation for constructing functional synthetic nanomachines. Rotaxane denotes a chemical structure consisting of a linear part and a cyclic part, tightly linked via noncovalent bonds within a complex structure. The difficult synthesis process of rotaxanes hinders their potential applications. One method for producing rotaxanes is through active template synthesis. Crown ethers are a perfect selection for inclusion in an active template strategy because of their extensively studied attributes and easy procurement in the market. Rotaxanes can be synthesized rapidly and easily through the use of Crown Ether Active Template Synthesis (CEATS). Simplifying the synthesis of rotaxanes will enable broader research and practical uses of these compounds. In this article through CEATS method rotaxane (5a) and (5b) is synthesized. Chemical structure of the obtained compounds was established by ^{1}HNMR, ^{13}CNMR and FT-IR spectroscopic methods.

1. Introduction

Over time, the historical development of isomeric varieties in organic molecules has progressed through significant stages: a) the molecules vary from one another in terms of their atom numbers and types; b) isomers with the usual arrangement and nature of bonding between these atoms; c) stereoisomers that are differentiated by their particular spatial sequence around or at the center of an atom; and d) topological isomers with different topological geometries. The last form of isomerism gives rise to mechanically interlocked molecules (MIMs), namely catenanes, rotaxanes, and knots, which take cues from various natural objects and architectures [1, 2]. For over half a century, chemists have dedicated their attention to creating MIMs. Their aesthetic beauty aside, their potential applications as molecular devices for information storage and processing make them truly remarkable. The rotaxane architecture, as one type of interlocked molecules, is deemed to be a versatile framework for building practical artificial nanomachines [3].

The synthesis of organic compounds containing nitrogen, sulfur, and oxygen, especially heterocycles, has long been a central focus in organic and supramolecular chemistry due to the unique chemical properties these elements impart [4-8]. Such compounds often display enhanced electronic characteristics, selective binding abilities, and catalytic activity, making them valuable building blocks in the design of functional materials, including interlocked molecular systems like rotaxanes. In particular, incorporating sulfur and nitrogen atoms into macrocyclic frameworks such as crown ethers can significantly influence host–guest interactions, stability, and synthetic efficiency in active-template approaches. Therefore, the use of N-, S-, and O-containing heterocycles opens promising avenues for constructing novel nanomachines with improved performance and structural versatility.

Molecular machines were the focus of the 2016 Nobel Prize in Chemistry for their design and synthesis. The emergence of interlocked molecular assemblies bonded by mechanical means has played a significant role in advancing molecular machinery, as acknowledged by the Nobel Committee. Currently, research in this field is

---

⁎ Corresponding author.; e-mail: mariamkh681@gmail.com

https://doi.org/10.22034/crl.2023.390623.1213

heavily focused on rotaxanes-molecules that are interlocked with a stoppered thread encircling a macrocycle [9].

The term rotaxane originates from the Latin terms for wheel and axle, referring to a compound composed of a linear part (also known as the rod-like component or guest) and a cyclic part (also known as the beadlike element or host), intricately connected through noncovalent forces in a threaded arrangement. Stoppers are bulky groups that can prevent dethreading of the cyclic component. In the absence of bulky stoppers at the end of the axle, the term pseudo- rotaxane implies that it is a false rotaxane, which does not qualify as a compound but rather as a supramolecular complex. Semi- rotaxane is a pseudo-rotaxane with only one stopper [10, 11].

The building blocks of rotaxane cannot be isolated without disrupting a covalent bond [12]; a variety of stimuli can adjust their relative positions effectively. Utilizing this unique property of rotaxanes has led to their significance as pumps, switchable catalysts [13], and electronic components [14].

Among the various types of macrocycles found in rotaxanes, crown ethers are highly abundant. This is mainly because they can establish strong complexes, like pseudo-rotaxanes, through the use of hydrogen bonding and π stacking with templates that have a range of functional groups, including secondary ammonium, urea, pyridinium, and amidinium [9].

As outlined in this article, a novel process for producing rotaxanes has been uncovered through crown ether active template synthesis (CEATS). CEATS maximizes the efficiency of reactions occurring within crown ethers. The synthesis process is made simpler by bypassing the necessity of establishing thermodynamically favored complexes between precursor components. A simple mixture of primary amine, crown ether, and electrophile in a non-polar solvent is all it takes for the spontaneous creation of rotaxane [15]. Proximity between the macrocycle and thread precursor components of rotaxane leads to accelerated reactions in active template synthesis. The key factor in achieving an effective active template reaction lies in stabilizing the transition state inside a macrocycle cavity, ultimately leading to the creation of a rotaxane as its kinetic product. Thus, passive template methods may be seen as operating based on thermodynamic control, while active template processes are governed by kinetic control [16]. The capability of employing this approach to speed up rotaxane construction was initially proven by Hirose and et al. [17], who illustrated the aminolysis of pre-rotaxane 4, which had a crown ether bonded to a stopper by means of a phenolic ester linkage, leading to the creation of rotaxane 5 with superior selectivity compared to non-interlocked thread.

Crown ethers are excellent options for utilization in an active template strategy due to their extensively studied properties and wide availability in the market. It has long been recognized that glymes and crown ethers play a key role in catalyzing various uncomplicated chemical reactions with amines, particularly ester aminolysis [18-20], nucleophilic aromatic substitution [21], and, more recently, ring-opening polymerization of N-carboxyanhydrides [22].

2. MTERIALS AND METHODS

2. 1. Synthesis of diamidic crown compound

Synthesis of sulfoxide (1) and methyl diester (2) synthesized in the previous article [23- 25].

Synthesis of 1,7-dioxa-10, 14-diaza-4-sulfoxo-9, 15-dioxo-2, 3, 5, 6 - di (´2,´4-dimethyl) benzo 16- crown-5 (3c):

For the synthesis of this reaction product under reflux in 20 ml of dry methanol solvent from the composition of methyl diester (2) (2 g, 0.0046 mol), 1,3-propanediamine (0.38 ml) to It was done for 12 hours. The completion of the reaction was monitored by TLC. The solvent inside the flask was removed by a rotary evaporator. and the remaining white slimy substance which then crystallized in methanol solvent and resulted in the formation of white cotton crystals. The reaction efficiency is 76% the melting point is 220-222 and R_f = 0.1-0.2 in the ethyl acetate/methanol (1:5) solvent system

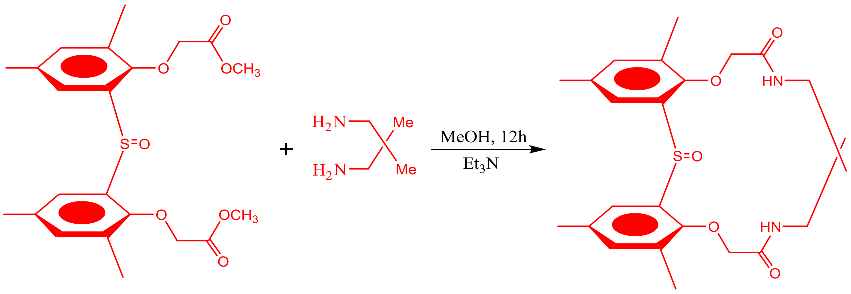

Scheme 1. Synthesis of diamidic crown compound (3c).

2.2. Synthesis of bis [N(((4-tert-butyl phenoxy) ethoxy) ethyl)] 4,4′-bipyridinium axel (4)

Axle synthesis involves two processes. During the initial stage,(20 mL) of acetonitrile were used to reflux (1 g, 0.2 mol) diethylene glycol ditosylate (0.886 g, 0.2 mol) 4-tert-butylphenol, and (0.384 g) of potassium carbonate reflaxed in 25 mL CH_3CN for 8 hours. Then rotary evaporator was used to extract the solvent. In 20 ML of $CHCl_3$ were used to remove the contents of the flask. The result was a white solid that crystallized in an ethanol. Subsequently,(0.2 g (1 mol) of 4,4′-bipyridinium and 0.615 g.) of the previous mixture were refluxed in 25 ml of DMF for 8 hours. After that, the solvent was rotary-evaporated. The substance was recrystallized in methanol and cotton white crystals was obtained.

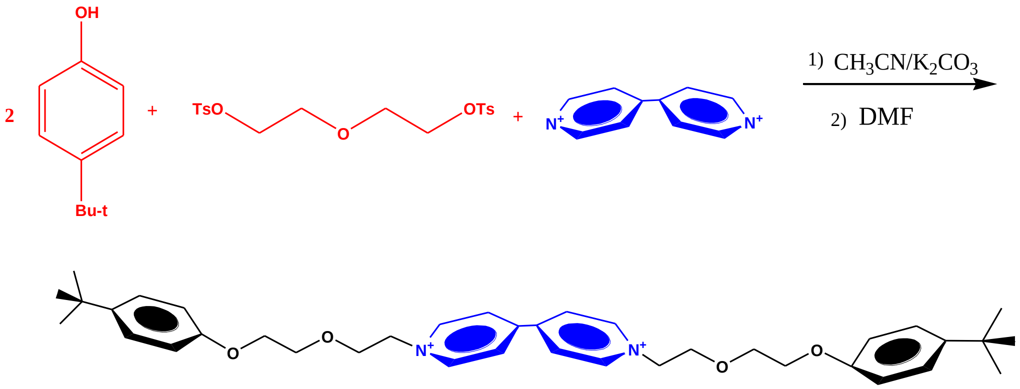

Scheme 2. preparation of axle.

2.3. Synthesis of rotaxane nanomachines

I. Synthesis of rataxane (5c) between axle and 1,7-dioxa-10, 14-diaza-4-sulfoxo-9, 15-dioxo-2, 3, 5, 6-('2,'4-dimethyl) di benzo 16- crown-5 (5c):

Axle and wheel (3c) with a molar ratio of 1:1 was refluxed in methanol for 10 hours in the presence of templating metal VCl_3 Then the solvent was removed by rotary and the material obtained was washed with hydrogenated water and distilled water. The obtained product crystallized in ethanol and resulted cotton-white crystals.

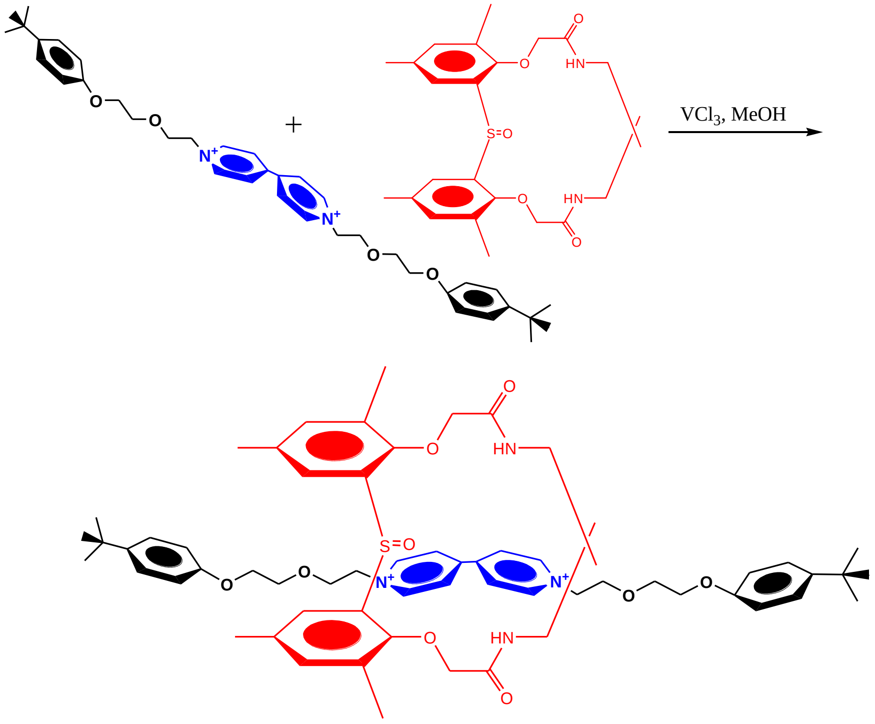

Scheme 3. Rotaxane (5c).

3. RESULTS AND DISCUSSION

IR spectra of Compound (3c) is shown in the Fig. 1S. The stretching vibrations related to the N-H bond in the region of 3397 cm^{-1} and the bending N-H bond in the region of 1510 cm^{-1} are seen with strong absorption. The absorption band of C=O at 1680 cm^{-1} is observed the ether C-O bond connected to the aromatic ring is in the region of 1120 cm^{-1} and the presence of the absorption band at 1671-1487 cm^{-1} is for the aromatic C=C bond. The aliphatic C-H bond which is in the region of 2900 cm^{-1} is shown as a slight absorption and the S=O bond is shown in the region of 1063 cm^{-1} which is a stretching vibration. Aromatic C-H bond in the 3100 cm^{-1} region and out-of-plane C-H bond in the 895 cm^{-1} region are observed as moderate absorption.IR spectra of Compound (4) is shown in the Fig. 2S. The aliphatic C-H bond that is slightly absorbed in the region of 2955 cm^{-1}. The aromatic stretching C-H bond is observed in the 3046 cm-1 region and the out-of-plane C-H bond is observed in the 814 cm^{-1} region as moderate absorption. The absorption bands observed at 1013, 1124 and 1213 cm-1 indicate ether bonds in C-O (aromatic), Ar-O-C and C-O-C.

IR spectrum of rotaxane (5c) is shown in Fig. 3.S [A], The presence of an absorption band at 1063 cm^{-1} indicates the S=O bond. The absorption band observed at 3397-3380 cm^{-1} is related to the stretching N-H bond and the bending N-H bond in the region of 1506-1510 cm^{-1} with strong absorption. C=O absorption band at 1680 cm^{-1}. Aliphatic C-H bond in the region of 2955-2900 cm^{-1} as a slight absorption. Aromatic C-H bond in the region of 3100-3046 cm^{-1} and out-of-plane C-H bond in the region of 895-814 cm^{-1} can be seen as moderate absorption. Absorption band at 1671-1487 cm-1 for aromatic C=C bond. The absorption bands observed at 1013, 1120, 1224 and 1213 cm^{-1} indicate ether bonds in C-O (aromatic) Ar-O-C and C-O-C. The peak observed in the region of 1360 cm^{-1} is for C-N.Fig. 4S. show ^1H NMR (A) and ^{13}C NMR (B) spectrums of compound (3c). The aromatic proton signals attributed to H_e and H_f reveal singlet peaks in the region of 6.98 and 7.21 ppm. The amide proton signal indicated a singlet peak at 7.59 ppm in related to H_g. The signals in the region of 1.12, 1.14, 2.21, and 2.23 ppm correspond to aliphatic methyl protons H_a, $H_{a'}$, H_d, and $H_{d'}$. At 4.67 ppm, H_c protons displayed a singlet peak. H_b indicates a singlet peak at 3.35 ppm. Signals of various carbon atoms demonstrate C_d (C=O) signal at 167.90 ppm, C_k at 152.08 ppm, C_l at 133.35 ppm, C_h at 131.93 ppm, C_g at 130.17 ppm, C_i at 121.76 ppm, C_j at 111.56 ppm, C_e at 66.94 ppm, C_c at 37.87 ppm, C_b at 34.68 ppm, C_f at 20.27 ppm, $C_{f'}$ at 20.57 ppm, C_a at 15.12 ppm and $C_{a'}$ at 15.55 ppm. A mass spectrum is obtained by electron impact (EI) at 70 eV. Peaks are detected at m/z (%): 480$(M)^+$, 481$(M+1)^+$, 482$(M+2)^+$, 356, 345, 331, 318, 302, 290, 276, 212, 198, 121, 106, 74, 73,58. Fig. 6S. show ^1H NMR (A) and ^{13}C NMR (B) spectrums of compound (4). Coupling H_e result in the doublet peaks at 6.78-6.80 ppm for the signals of aromatic protons detect by H_f. Doublet peaks in the region of 7.15–7.17 ppm indicates signals from H_e that were coupling with H_f. At 8.89–8.91 ppm, doublet peaks are observed for H_h signals due to their coupling with H_g. Doublet peaks at 9.31–9.33 ppm indicate signals from H_g that are coupling with H_h. A mass spectrum is obtained by electron impact (EI) at 70 eV. Fig. 8S. show ^1H NMR (A) and ^{13}C NMR (B) spectrums of compound (5c). The aromatic proton signals indicate a singlet peak at 6.98 and 7.21 ppm in related to H_e and H_f. Doublet peaks at 6.78-6.80, 7.15-7.17, 8.89-8.91 and 9.31-9.33 ppm indicate signals from H_j that are coupling with $H_{i,}$ H_i that are coupling with $H_{j,}$ H_p that are coupling with H_o and H_o that are coupling with H_p, respectively. The amide proton signal indicates a singlet peak at 7.59 ppm. The aliphatic proton signals attribute to H_a and $H_{a'}$ reveal singlet peaks in the region of 1.12 and 1.14 ppm, respectively. At 1.35 ppm, singlet peaks are observed for H_h signals. At 2.21, 2.23, 3.25 and 4.67 ppm, singlet peaks are observed for H_d, $H_{d'}$, H_b and H_c signals, respectively [26-28]. A mass spectrum is obtained by electron impact (EI) at 70 eV.

3.1. Surface morphology

The morphology of compound (5c) was investigated through scanning electron microscopy (SEM) experiments. According to Figure 1 the images show the formation of randomly scattered rectangular structures with diameters of 26 to 98 nm. The main advantage of this synthesis method is its ability to produce particles in nano dimensions without depending on the traditional methods that are usually used for the synthesis of nanostructures[29].

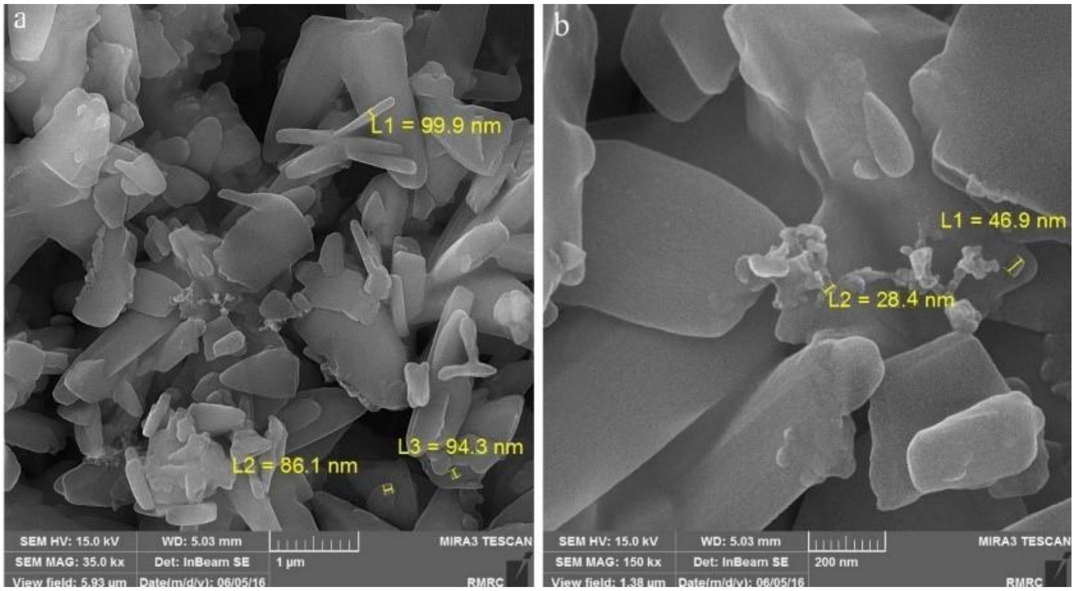

Figure 1. FESEM image of rotaxane (5c)

4. Conclusions

Over the last several years, crown ether active template synthesis (CEATS) has emerged as a simple and effective way to synthesis rotaxanes. This strategy takes advantage of crown ethers capacity to expedite basic organic reactions. Systems Chemists have the exciting opportunity to develop responsive nanotechnology and transient materials by integrating chemical reaction networks with rotaxane (dis)assembly, including transient Fmoc protection and transamidation. We predict that CEATS will serve as a crucial method for enhancing the creation of intricate molecular machinery and discovering dynamic molecular structures not yet explored.

References

[1] a) H. H. Wasserman, J. J. Keggi, J. E. McKeon, Serratamolide, a metabolic product of Serratia. *Journal of the American Chemical Society*, 83 (1961) 4107-4108; b) G. A. Breault, C. A. Hunter, P. C. Mayers, Supramolecular topology. *Tetrahedron*, 55 (1999) 5265-5293; c) R. S. Forgan, J.-P. Sauvage, J. F. Stoddart, Chemical topology: complex molecular knots, links, and entanglements. *Chemical Reviews,* 111 (2011) 5434-5464.

[2] a) S. Li, H. Jianying, P.J. Bryant, K. Hyunuk, C. Ki-Whan, Formation of [3] catenanes from 10 precursors via multicomponent coordination-driven self-assembly of metallarectangles. Journal of the American Chemical Society, 135 (2013) 2084-2087; b) S. Li., J. Huang, F. Zhou, T.R. Cook, X. Yan, Y. Ye, B. Zhu, B. Zheng, P.J. Stang, Self-assembly of triangular and hexagonal molecular necklaces. *Journal of the American Chemical Society,* vol. 136, (2014) 5908-5911.

[3] a) V. Balzani, A. Credi, M. Venturi, Molecular devices and machines. *Nano Today*, 2 (2007) 18-25; b) W. Yang, Y. Li, H. Liu, L. Chi, Y. Li, Design and Assembly of Rotaxane-Based Molecular Switches and Machines, *Small*, 8 (2012) 504-516.

[4] a) M. Ghaghaei, M. Babazadeh, F. Behmagham, L. Edjlali, E. Vessally, A theoretical evaluation for new fused remote N-heterocyclic silylenes (RNHSis) using density functional theory, *Journal of Physical Organic Chemistry* (2023) e4475, 10.1002/poc.4475; b) S. Majedi, L. Sreerama, E. Vessally, F. Behmagham, Metal-free regioselective thiocyanation of (hetero) aromatic CH bonds using ammonium thiocyanate: an overview, *Journal of Chemistry Letters*, 1(1) (2020) 25-31; c) F. Zarei, S. Soleimani-Amiri, Z. Azizi, Heterogeneously Catalyzed Pechmann Condensation Employing the $HFe(SO_4)_2.4H_2O$-Chitosan Nano-Composite: Ultrasound-Accelerated Green Synthesis of Coumarins, *Polycyclic Aromatic Compounds*, 42 (2022) 6072-6089, 10.1080/10406638.2021.1973520; d) S.F. Taheri Hatkehlouei, B. Mirza, S. Soleimani-Amiri, Solvent-free one-pot synthesis of diverse dihydropyrimidinones/tetrahydropyrimidinones using biginelli reaction catalyzed by Fe_3O_4@C@OSO_3H, *Polycyclic Aromatic Compounds*, 42 (2022) 1341-1357, 10.1080/10406638.2020.1781203.

[5] a) I. S. Hasan, A. A. Majhool, M. H. Sami, M. Adil, S. S. S. A. Azziz, DFT Investigation of structure, stability, NBO charge on Titanium—Nitrogen nanoheterofullerenes evolved from a small nanocage, *Chemical Review and Letters*, 6 (2023), 10.22034/crl.2023.392371.1223; b) E. Ezzatzadeh, S. Soleimani-Amiri, Z. Hossaini, K. Khandan Barani, Synthesis and evaluation of the antioxidant activity of new spiro-1,2,4-triazine derivatives applying Ag/Fe_3O_4/CdO@MWCNT MNCs as efficient organometallic nanocatalysts, *Frontiers in chemistry*, 10 (2022) 1001707, 10.3389/fchem.2022.1001707; c) H. Ghavidel, B. Mirza, S. Soleimani-Amiri, M. Manafi, New insight into experimental

and theoretical mechanistic study on a green synthesis of functionalized 4H-chromenes using magnetic nanoparticle catalyst, *Journal of the Chinese Chemical Society*, 67 (2020) 1856-1876, 10.1002/jccs.201900554; d) S. Soleimani-Amiri, Z. Hossaini, Z. Azizi, Synthesis and Investigation of Biological Activity of New Oxazinoazepines: Application of Fe_3O_4/CuO/ZnO@MWCNT Magnetic Nanocomposite in Reduction of 4-Nitrophenol in Water, *Polycyclic Aromatic Compounds*, 43 (2022) 2938-2959, 10.1080/10406638.2022.2058969.

[6] a) F. Iorhuna, A. S. Muhammad, A. M. Ayuba, A. T. Nyijime, Molecular Dynamic Simulations and Quantum Chemical Studies of Nitrogen Based Heterocyclic Compounds as Corrosion Inhibitors on Mild Steel Surface, *Chemical Review and Letters*, 6 (2023) 114-127. 10.22034/crl.2023.400989.1226; b) E. Hemmati, S. Soleimani-Amiri, M. Kurdtabar, A CMC-*g*-poly(AA-co-AMPS)/Fe_3O_4 hydrogel nanocomposite as a novel biopolymer-based catalyst in the synthesis of 1,4-dihydropyridines, *RSC Advances*, 13 (2023) 16567-16583, 10.1039/D3RA01389H; c) M. Feizpour Bonab, S. Soleimani-Amiri, B. Mirza, Fe_3O_4@C@PrS-SO_3H: A Novel Efficient Magnetically Recoverable Heterogeneous Catalyst in the Ultrasound-Assisted Synthesis of Coumarin Derivatives, *Polycyclic Aromatic Compounds*, 43 (2023) 1628-1643, 10.1080/10406638.2022.2032768; d) A.K.O. Aldulaimi, M.J. Jawad, S.M. Hassan, T.S. Alwan, S.S.S.A. Azziz, Y M. Bakri, The potential antibacterial activity of a novel amide derivative against gram-positive and gram-negative bacteria. *International Journal of Drug Delivery Technology*, 12(2) (2022) 510-515 doi:10.25258/ijddt.12.2.8.

[7] a) M. Koohi, H. Bastami, Investigation of Ti—B nanoheterofullerenes evolved from C20 nanocage through DFT, *Chemical Review and Letters*, 6 (2023) 223. 10.22034/crl.2023.392356.1222; b) S. Soleimani Amiri, Green production and antioxidant activity study of new pyrrolo[2,1-a]isoquinolines, *Journal of Heterocyclic Chemistry*, 57 (2020) 4057-4069, 10.1002/jhet.4115; c) A. K. O. Aldulaimi, A. H. Idan, A. A. Majhool, M. J. Jawad, Z. H. Khudhair, S. M. Hassan, S. S. S. A. Azziz, Synthesis of new antibiotic agent based on mannich reaction. *International Journal of Drug Delivery Technology*, 12(3) (2022) 1428-1432. doi:10.25258/ijddt.12.3.83; d) M. N. Sidik, Y. Mhd Bakri, S. S. Syed Abdul Azziz, A. K. O. Aldulaimi, C. F. Wong, M. Ibrahim, In silico xanthine oxidase inhibitory activities of alkaloids isolated from alphonsea, *South African Journal of Botany*, 147 (2022) 820-825. doi:10.1016/j.sajb.2022.03.024.

]^] a) A.K.O. Aldulaimi, M.J. Jawad, S.M. Hassan, T.S. Alwan, S.S.S.A. Azziz, Y M. Bakri, The potential antibacterial activity of a novel amide derivative against gram-positive and gram-negative bacteria, *Journal of Heterocyclic Chemistry*, 12(2) (2022) 510-515 doi:10.25258/ijddt.12.2.8; b) C.Y. Hsu, A.K.O. Aldulaimi, H. Bahair, A.H. Adhab, S.K. Saraswat, Hydrazinosulfonylation of aryl electrophiles: a straightforward approach for the synthesis of aryl N-aminosulfonamides, *RSC Advances*, 13(27) (2023) 18546-18560, 10.1039/D3RA03123C, c) J. Radhi, Inam, A. Al-Khafagi, Ahmed, K. Kahlol, Mohammed, Mashkoor, S. Muthana, 1,2-Naphthaquinolinc-4-Sulphonate Sodium as Reagent for Spectrophotometric Determination of Rivoglitazone, *International Journal of Drug Delivery Technology*, 11(4) (2021) 1146 – 1149, 10.25258/ijddt.11.4.5.

[9] a) O. Ramström, Scientific background on the nobel prize in chemistry 2019. *The Royal Academy of Sciences*, (2019); b) C. J. Bruns J. F. Stoddart, The nature of the mechanical bond: from molecules to machines. (2016).

[10] I. T. Harrison, S. Harrison, Synthesis of a stable complex of a macrocycle and a threaded chain. *Journal of the American Chemical Society*, 89 (1967) 5723-5724.

[11] M. Xue, Y. Yang, X. Chi, X. Yan, F. Huang, Development of pseudorotaxanes and rotaxanes: from synthesis to stimuli-responsive motions to applications. *Chemical reviews*, 115 (2015) 7398-7501.

[12] J. S. Seale, Y. Feng, L. Feng, R. D. Astumian, J. F. Stoddart, Polyrotaxanes and the pump paradigm. *Chemical Society Reviews*, 51 (2022) 8450-8475.

[13] C. Kwamen, J. Niemeyer, Functional rotaxanes in catalysis. *Chemistry–A European Journal*, 27 (2021) 175-186.

[14] P. Wu, B. Dharmadhikari, P. Patra, X. Xiong, Rotaxane nanomachines in future molecular electronics. *Nanoscale Advances*, 4 (2022) 3418-3461.

[15] S. D. Fielden, Crown ether active template synthesis of rotaxanes. *ChemSystemsChem*, 6 (2024) e202300048,.

[16] M. Denis, S. M. Goldup, The active template approach to interlocked molecules. *Nature Reviews Chemistry*, 1 (2017) 0061.

[17] K. Hirose, K. Nishihara, N. Harada, Y. Nakamura, D. Masuda, M. Araki, Y. Tobe, Highly selective and high-yielding rotaxane synthesis via aminolysis of prerotaxanes consisting of a ring component and a stopper unit, *Organic Letters*, 9 (2007) 2969-2972.

[18] J. C. Hogan, R. D. Gandour, Structural requirements for glyme catalysis in butylaminolysis of aryl acetates in chlorobenzene. Identification of-OCH2CH2OCH2CH2OCH2CH2O-as the optimal subunit for catalysis. *The Journal of Organic Chemistry*, 56 (1991) 2821-2826.

[19] J. C. Hogan, R. D. Gandour, Fingerprinting a transition-structure guest by a building-block approach with an incremental series of catalytic hosts. Structural requirements for glyme and. alpha.,. omega.-dimethoxyalkane catalyses in N-methylbutylaminolysis and butylaminolysis of 4-nitrophenyl acetate in chlorobenzene. *The Journal of Organic Chemistry*, 57 (1992) 55-61.

[20] N. Basilio, L. García-Río, J. C. Mejuto, M. Pérez-Lorenzo, A new reaction pathway in the ester aminolysis catalyzed by glymes and crown ethers, *The Journal of Organic Chemistry*, 71 (2006) 4280-4285.

[21] N. Basilio, L. García-Río, Á. Peña-Gallego, M. Perez-Lorenzo, Molecular recognition-based catalysis in nucleophilic aromatic substitution: a mechanistic study. *New Journal of Chemistry*, 36 (2012) 1519-1526.

[22] Y. Xia, Z. Song, Z. Tan, T. Xue, S. Wei, L.Zhu, Y. Yang, Accelerated polymerization of N-carboxyanhydrides

caAccelerated polymerization of N-carboxyanhydrides catalyzed by crown ether. *Nature communications,* 12 (2021) 732.

[23] A. Najdhashemi, S. Bavili Tabrizi, M. Babazadeh, Synthesis and characterization of new rotaxanes from related crown compounds. *Journal of Inclusion Phenomena and Macrocyclic Chemistry,* (2024) 1-23.

[24] A. Shockravi, R. Alizadeh, H. Aghabozorg, A. Moghimi, E. Rostami, S. Bavili, Synthesis and crystal structure determination of 2, 2′-sulfinyl-bis (4-methyl phenol) and 2, 2′-thio-bis (4-methyl phenol). *Phosphorus, Sulfur, and Silicon*, 178 (2003) 2519-2527.

[25] A. Shockravi, S. Bavili T, E. Rostami, A. Yousefi, A. Dehjurian, R. Tohidi, Synthesis of new dibenzosulfide and dibenzosulfoxide macrocyclic compounds. *Journal of inclusion phenomena and macrocyclic chemistry,* 49 (2004) 163-166.

[26] Y. Akae, Y. Koyama, H. Sogawa, Y. Hayashi, S. Kawauchi, S. Kuwata, T. Takata, Structural Analysis and Inclusion Mechanism of Native and Permethylated α-Cyclodextrin-Based Rotaxanes Containing Alkylene Axles, *Chemistry–A European Journal,* 22 (2016) 5335-5341.

[27] Y. Akae, H. Sogawa, T. Takata, Effective synthesis and modification of α-cyclodextrin-based [3] rotaxanes enabling versatile molecular design. *European Journal of Organic Chemistry*, 2019 (2019) 3605-3613.

[28] Y. Akae, T. Takata, O-Acylative Vinylation of Cyclodextrin-Based [3] Rotaxane Towards Rotaxane Crosslinkers, *European Journal of Organic Chemistry*, 26 (2023) e202300009.

[29] Y. Akae, P. Theato, Aggregation Behavior of Cyclodextrin-Based [3] Rotaxanes. *Chemistry–A European Journal*, 29 (2023) e202301582.